Journal of the Korean Magnetic Resonance Society **1998**, *2*, 1-23

^{13}C Spin-Lattice Relaxation Study of Segmental Motions in *n*-alkanes : *n*-Undecane and *n*-Dodecane

Buem Chan Min and Jo Woong Lee*

Department of Chemistry, Seoul National University
Received January 13, 1998

Abstract : The motions of carbon-chain backbone in *n*-undecane and *n*-dodecane dissolved in $CDCl_3$ are investigated by ^{13}C NMR relaxation study. For this purpose a model of C – C backbone motions for these molecules is introduced that takes into account the cooperativities between rotations about two β-coupled C – C bonds. In this model it is assumed that the major conformational interconversions occurring in the inner part of the chain involve the type II jumps only, although at terminal part of the chain both type II and type III motions are assumed to take place. Information of the rate constants for these conformational transitions could be extracted by comparing the T_1's calculated on the basis of the assumed model with those observed over the temperature range of 248 - 308K. The calculations were performed according to the method proposed by Wittebort and Szabo. The activation energies, ranging from *ca* 12 to 20 kJ/mol, could be obtained from the Arrhenius plots of these calculated rate constants.

Recently, there have been vigorous efforts to elucidate the details of the chain dynamics for molecules of moderate chain length[1-6], such as *n*-alkanes, in liquid because such study can help us understand their molecular properties related to the chain motions in condensed phase. In a previous paper[2] we have investigated the carbon backbone motions in several *n*-alkanes dissolved in $CDCl_3$, ranging from *n*-octane to *n*-dodecane, *via* measurement of ^{13}C T_1's and subsequent interpretation of these data on the basis of two crude theoretical models, Wallach's multiple internal rotation model[7] and the London-Avitabile jump model[3]. These models assume that the internal rotations about different C – C bonds in the chain are mutually independent and, as such, can provide no way to study the cooperativities among these internal rotations. Therefore, we feel that they need further refinement to accommodate the cooperativities among internal rotations about different

C – C bonds in proximity to each other.

Experiments show that in liquid or solution state the activation energies for segmental motions in many polymeric chain molecules are only slightly higher than those of one bond rotation in small molecules[8-10]. These results have been accepted as an evidence that internal rotation of a chain segment about a C – C bond occurs in such a way that the other parts of the molecule simultaneously undergoes rotation about another C - C bond that is β-coupled to the first C - C bond, thereby reducing the inhibition due to the viscous drag force by the solvent molecules. The objective of this study is to explore a method of incorporating the idea of this cooperativity into such a simple model as the London–Avitabile jump model[3] and apply it to interpret the ^{13}C T_1 data for two hydrocarbon molecules, *n*-undecane and *n*-dodecane. Although some investigators prefer the model free approach [4,5,11], we still feel that the approach based on a simple model has some merits in that it is not only mathematically tractable but also provides a clear and instructive, though qualitative, picture of the elementary processes making up the complicated segmental motions occurring in the chain.

Models for Describing Segmental Motions in Chain Molecules

In various models proposed thus far it is customary to assume that the global motions of a chain molecule in solution proceed by diffusive steps while the local segmental motions along the chain are of either diffusive or jumping character [3,7,12-17]. Wallach[7] assumed in his early study of segmental motions in chain molecules that all the internal rotations about C - C bonds were diffusive and independent of one another. Later, London and Avitabile[3] considered each internal rotation about C - C bond occurring as a result of independent jumps among three states, g^+, t, g^- with the restriction that direct $g^+ \leftrightarrow g^-$ transitions be forbidden. Helfand[10,18] has classified the conformational transitions in the chain molecules into three types, which will be referred to as type I, II, and III hereafter, as shown in Fig.1. In type I transitions both ends of the segment undergoing the conformational transition remain fixed before and after the transition. Undoubtedly, the activation energy of this type of motion must be large since it involves the energy of at least two barrier crossings plus the solvent frictions. In type III transition, relative orientation of one end of the segment undergoing transition changes with respect to the other end as a result of this transition. This type of motion can have low activation energy for an isolated molecule but in condensed phase it normally occurs very slowly because of large frictional forces exerted by solvent molecules. However, it is well known that even for long polymer molecules the observed activation energy of segmental motions is comparable to or only slightly higher than that of single barrier crossing in small molecules. This observation can readily be understood if we

assume the presence of type II transitions, because when a segment undergoes this type of transitions by changing the conformation of a given C - C bond, other C - C bonds β-coupled to it can readjust their conformations so that the solvent friction forces suffered by the attached groups swinging through large volumes of solvent may be greatly reduced. In accord with this Helfand has concluded through his computer simulation study that the conformational transitions of type II occur very frequently in the long chain molecules in liquid[9,19,20]. He has also mentioned that isolated-type motions can also occur as frequently as type II transitions but these type of motions may not be considered as complete conformational changes in the usual sense. They are just temporal distortions of the stable conformations lasting for very short period ($\sim 10^{-12}$ sec) which in most cases simply return to the original equilibrium conformations[20]. This short-time local mode motions, which are frequently referred to as liberations, are known to reduce the effectiveness of dipole-dipole interaction as a relaxation mechanism as shown by Ediger *et al.*[21]. When this type of motions plays substantial role, their effects are manifested through the T_1 *vs* $1/T$ curve showing distinctive minima which are shallower than they would be otherwise. It seems that these liberational effects are more pronounced when the segment involved in the motion is anchored at both ends by heavier molecular moieties.

The two hydrocarbons we are considering, *n*-undecane and *n*-dodecane, have relatively short carbon chains which are open at both ends and do not always show the behaviors characteristic of long-chain polymer molecules of high molecular weight whose chain segments are usually heavily anchored at both ends. For these hydrocarbons dissolved in $CDCl_3$ all the carbon lines are well resolved (in 50 and 125MHz ^{13}C spectra) and the NOE factors for these lines are all found to be very close to their maximum (≈ 1.987) over the entire range of experimental temperature, which indicates that the extreme narrowing condition is very well valid in these cases. Further, T_1 values for all the carbons are found to monotonously decrease as temperature is lowered, displaying no minima whatsoever across the entire range of observed temperature. Even at the lowest limit of the investigated temperature range no sign could be found that any minima would soon be reached. This suggests that rapid liberational motions with very short correlation time can make only trivial contributions to T_1 in these molecules. Molecular dynamics calculations reported by Evans and Knauss[22], Grant and coworkers[23], and Smith and Yoon[24] also suggest that this is indeed the case for *n*-alkanes of moderate chain length. Thus we may conclude that for *n*-undecane and *n*-dodecane the major contributions to T_1 come from the jumps among the stable conformations and the overall molecular rotations.

Then, what types of the Helfand transitions are possible for *n*-undecane and *n*-dodecane? First, type I mode of transitions must be excluded from our consideration because the above two hydrocarbons, unlike the long-chain polymer molecules, do not have the

chains lengthy enough to sustain this type of motions. Type I transition such as the crankshaft motion could easily turn into overall rotation of the entire molecule along the long axis of the chain. Thus we have to be concerned only with type II and type III transitions. As we shall explain later, with type II or type III motions alone the observed T_1 data cannot faithfully be reproduced over the range of experimental temperatures. This means that both of these two types of motions should be combined together to explain the observed behaviors of T_1 in *n*-undecane and *n*-dodecane. How can we construct a model of chain dynamics comprised of these two types of motions that can explain all the observed results satisfactorily? Helfand's works[19, 20] give us the hint that in inner part of the chain the type II motions, such as pair *gauche* generation and *gauche* migration, will prevail over the type III motions due to the presence of viscous drag forces exerted on the molecular part swinging through the solvent. However, as we move toward the terminal side, the latter motions play increasingly more important roles since the viscous drag force due to the solvent will gradually decrease. Thus, near the chain end we probably would have to take both of these two types of motions together into consideration to construct our model of local chain dynamics. In the present work several models consistent with this picture have been contrived and tested for the observed T_1 data. It turned out that not all the models yielded the physically acceptable consequences. As we shall describe later, the model which seems to be most consistent with the physical reality is the one in which inner part of the chain undergoes only the type II jumps while for terminal ethyl and propyl groups both type II and type III jumps are possible. This model can, of course, be more rigorously tested and refined if experimental data other than T_1 become available through sophisticated experiments such as coupled relaxation measurement.

Investigation of molecular dynamics by NMR spectroscopy usually requires the measurement of relaxation parameters such as T_1, T_2 and NOE factor. If dipole–dipole interaction between ^{13}C and ^{1}H directly bonded to each other provides the dominant relaxation pathway, T_1 for ^{13}C of interest under the condition of broadband proton decoupling may be written as follows[3,15]:

$$\frac{1}{T_1} = \left(\frac{N_H}{20}\right)\left(\frac{\mu_0 \gamma_C \gamma_H \hbar}{4\pi r_{CH}^3}\right)^2 \left[J(\omega_C - \omega_H) + 3J(\omega_C) + 6J(\omega_C + \omega_H)\right], \qquad (1)$$

where N_H is the number of protons directly bonded to the carbon of interest, μ_0 is the magnetic permeability constant, γ_H and γ_C are, respectively, the magnetogyric ratios of ^{1}H and ^{13}C nuclei, and r_{CH} represents the distance between directly bonded ^{13}C and ^{1}H.
The spectral density, $J(\omega)$ appearing in Eq.(1), is defined as follows :

$$J(\omega) = \int_{-\infty}^{\infty} G(\tau)\exp(-i\omega\tau)d\tau \ , \qquad (2)$$

where $G(\tau)$ is a time-dependent correlation function for the carbon of interest that can be expressed in terms of the second-order Wigner rotation matrix elements as [7,25]

$$G(\tau) = 5\left\langle D_{q0}^{(2)*}(\Omega^0)\, D_{q0}^{(2)}(\Omega^\tau)\right\rangle \qquad (3)$$

with Ω^τ denoting the orientation of ^{13}C – ^{1}H bond at time τ with respect to the laboratory-fixed coordinates.

For systematic description of the problem we introduce the three coordinate systems as shown in Fig. 2. In the followings brief descriptions of them are given:

$\left(X_L, Y_L, Z_L\right)$: A laboratory-fixed coordinates system with the static magnetic field B_0 directed along the Z_L axis. Referred to as the L-coordinates hereafter;

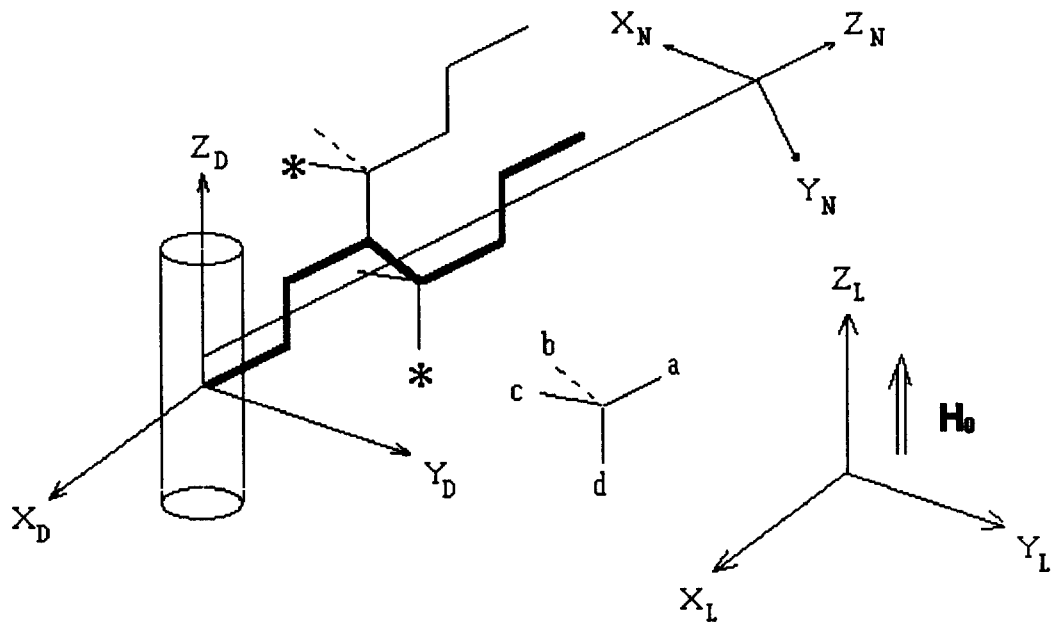

Fig. 2. The coordinate system for describing the segmental motions in a chain molecule

(X_D, Y_D, Z_D): A body-fixed coordinates system with the two of the coordinates axes(X_D and Z_D) lie on the plane that involves the innermost carbon and, at the same time, bisects the bond angle $\angle$HCH at this carbon site. The Z_D axis is taken along the symmetry axis of all *trans* conformer. The third axis, Y_D, is taken as perpendicular to this plane.

(X_N, Y_N, Z_N): A coordinates properly chosen for convenient description of the $^{13}C - {}^{1}H$ internuclear vector of interest. In our case the Z_N axis is chosen along the first C – C bond protruding from the innermost carbon. Referred to as the N-coordinates hereafter.

The change of orientation of $^{13}C - {}^{1}H$ bond accompanying a conformational transition is also shown in the same figure. With these coordinates properly defined the overall rotation of the molecule is conveniently described as the change of orientation of (X_D, Y_D, Z_D) coordinates with respect to the laboratory-fixed coordinates (X_L, Y_L, Z_L) and the motion of the $^{13}C - {}^{1}H$ vector of interest can easily be dealt with by looking at the movement of the (X_N, Y_N, Z_N) coordinates with respect to the (X_D, Y_D, Z_D) coordinates. Successive transition from the (X_L, Y_L, Z_L) coordinates to the (X_D, Y_D, Z_D) coordinates and, finally, to the (X_N, Y_N, Z_N) coordinates can be effected by the following transformation:

$$D^{(2)}_{q0}(\Omega_{LF}) = \sum_{a,b} D^{(2)}_{qa}(\Omega_{LD}) D^{(2)}_{ab}(\Omega_{DN}) D^{(2)}_{b0}(\Omega_{CH}), \qquad (4)$$

where Ω_{LD} denotes a set of the three Euler angles describing the orientation of the D–coordinates with respect to the L–coordinates while Ω_{DN} is the set of those angles describing the orientation of the N–coordinates with respect to the D–coordinates. (See Fig. 2.) Likewise, the symbol Ω_{CH} stands for the set of three Euler angles describing the orientation of the CH bond vector of interest with respect to the N-coordinates system. In our case we choose the N-coordinates such that the orientation Ω_{DN} does not depend on time. Furthermore we can take one of the Euler angle γ_{DN} as zero. Then, substitution of Eq.(4) into Eq.(3) and assumption that the fluctuation of Ω^t_{LD} is independent of that of Ω^t_{CH} lead us to the expression

$$G(\tau) = 5 \sum_{a,a',b,b'} \left\langle D_{qa}^{(2)*}\left(\Omega_{\mathrm{LD}}^{0}\right) D_{qa'}^{(2)}\left(\Omega_{\mathrm{LD}}^{\tau}\right)\right\rangle \exp\left[i(a-a')\alpha_{\mathrm{DN}}\right] \times d_{ab}^{(2)}\left(\beta_{\mathrm{DN}}\right) d_{a'b'}^{(2)}\left(\beta_{\mathrm{DN}}\right)\left\langle D_{b0}^{(2)*}\left(\Omega_{\mathrm{CH}}^{0}\right) D_{b'0}^{(2)}\left(\Omega_{\mathrm{CH}}^{\tau}\right)\right\rangle . \tag{5}$$

Under the simplifying condition that the rotation of D-coordinates frame with respect to the laboratory-fixed frame can be described by rotational diffusion of a prolate top $\left\langle D_{qa}^{(2)*}\left(\Omega_{\mathrm{LD}}^{0}\right) D_{qa'}^{(2)}\left(\Omega_{\mathrm{LD}}^{\tau}\right)\right\rangle$ may be written as follows:

$$\left\langle D_{qa}^{(2)*}\left(\Omega_{\mathrm{LD}}^{0}\right) D_{qa'}^{(2)}\left(\Omega_{\mathrm{LD}}^{\tau}\right)\right\rangle = \frac{1}{5}\exp\left\{-\left[6D_{\perp} + a^{2}\left(D_{//} - D_{\perp}\right)\right]\tau\right\}\delta_{aa'}, \tag{6}$$

where $D_{//}$ and $D_{\perp}$ are, respectively, the principal component of rotational diffusion tensor **D** parallel with and perpendicular to the symmetry axis of the assumed prolate top.

Substitution of Eq.(6) into Eq.(5) leads to

$$G(\tau) = \sum_{a,b,b'} \exp\left(-\left\{6D_{\perp} + a^{2}\left(D_{//} - D_{\perp}\right)\tau\right\}\right) d_{ab}^{(2)}(\beta_{\mathrm{DN}}) d_{ab'}^{(2)}(\beta_{\mathrm{DN}}) \times \left\langle D_{b0}^{(2)*}(\Omega_{\mathrm{CH}}^{0}) D_{b'0}^{(2)}(\Omega_{\mathrm{CH}}^{\tau})\right\rangle, \tag{7}$$

where β_{DN} is the angle that the Z_{D} axis makes with the Z_{N} axis. The correlation function $\left\langle D_{b0}^{(2)*}(\Omega_{\mathrm{CH}}^{0}) D_{b'0}^{(2)}(\Omega_{\mathrm{CH}}^{\tau})\right\rangle$ can be calculated if the conditional probability $p\left(k,\tau \middle| l,0\right)$ that the C - C chain, existing initially in l conformation, assumes k conformation at a later time τ is known. That is,

$$\left\langle D_{b0}^{(2)*}\left(\Omega_{\mathrm{CH}}^{0}\right) D_{b'0}^{(2)}\left(\Omega_{\mathrm{CH}}^{\tau}\right)\right\rangle = \sum_{k,l} \exp\left(ib\alpha_{\mathrm{CH}}^{l}\right) d_{b0}^{(2)}\left(\beta_{\mathrm{CH}}^{l}\right) p_{\mathrm{eq}}(l) \times \exp\left(-ib'\alpha_{\mathrm{CH}}^{k}\right) d_{b'0}^{(2)}\left(\beta_{\mathrm{CH}}^{k}\right) p\left(k,\tau \middle| l,0\right), \tag{8}$$

where $p_{\mathrm{eq}}(l)$ is the probability that the chain is found in l conformation at thermal equilibrium and the summation in Eq.(8) runs over all the possible conformations. α_{CH}^{l} and β_{CH}^{l} stand for the azimuthal and the polar angle, respectively, of the ^{13}C – ^{1}H bond of interest in l conformation with respect to the N–coordinate system. Fig. 2, for example, shows α_{CH}^{l} and β_{CH}^{l} for the ^{13}C – ^{1}H bond in $tttt$ and $tg^{+}tg^{-}$ conformation (each

marked by an asterisk). If the conformational change in the chain proceeds by jumping among M conformers, the conditional probability $p(k,\tau \mid l,0)$ can be calculated by the method due to Wittebort and Szabo[15]. For our further discussion their method will be briefly outlined in what follows.

Wittebort and Szabo started from the following first-order kinetic equation:

$$(\partial/\partial t)p_i(t) = \sum_j \tilde{R}_{ij}\, p_j(t) \ , \tag{9}$$

where $p_i(t)$ is the probability that the chain is found to exist in i conformation at time t and $\tilde{R}_{ij}$ is the rate constant for the conformational jump $j \rightarrow i$ with $\tilde{R}_{ii} = -\sum_{j(\neq i)} \tilde{R}_{ji}$. To obtain conditional probability $p(k,\tau \mid l,0)$ it is necessary to solve these coupled differential equations. In general, the solutions to the coupled linear differential equations like Eq.(9) may be written in the form

$$p_j(t) = \sum_k \tilde{X}_{jk} \exp(-\lambda_k t) \ . \tag{10}$$

Substitution of Eq.(10) into Eq.(9) leads to an eigenvalue equation

$$\tilde{\mathbf{R}}\tilde{\mathbf{X}} = -\lambda\tilde{\mathbf{X}} \ . \tag{11}$$

The rate matrix $\tilde{\mathbf{R}}$ is in general not symmetric since two rate constants $\tilde{R}_{ij}$ and$\tilde{R}_{ji}$ are not necessarily equal to each other. Thus, to effect the diagonalization of $\tilde{\mathbf{R}}$ we have to introduce the following transformations to convert Eq.(11) to an eigenvalue equation for a symmetric matrix $\mathbf{R}$:

$$R_{ij} = \left(\tilde{R}_{ij}\tilde{R}_{ji}\right)^{1/2}, \ X_i = \left[p_{\mathrm{eq}}(i)\right]^{-1/2}\tilde{X}_i \ . \tag{12}$$

These relations, together with the microscopic reversibility condition $\tilde{R}_{ij}p_{\mathrm{eq}}(j) = \tilde{R}_{ji}p_{\mathrm{eq}}(i)$, lead us to

$$\mathbf{RX} = -\lambda\mathbf{X} \tag{13}$$

which is an eigenvalue equation for a symmetric matrix $\mathbf{R}$.

It can be shown[15] that $p_{eq}(l)$ and $p(k,\tau|l,0)$ may be expressed in terms of eigenvalues and eigenvectors for Eq.(13) as follows:

$$X_i^{(0)} = \left[p_{eq}(i)\right]^{1/2} \tag{14}$$

and

$$p(k,\tau|l,0) = X_k^{(0)}\{X_l^{(0)}\}^{-1}\sum_n X_k^{(n)}X_l^{(n)}\exp(-\lambda_n\tau), \tag{15}$$

where $X_l^{(0)}$ and $X_l^{(n)}$ are the lth element of the eigenvectors corresponding to the eigenvalues $\lambda_0(=0)$ and λ_n, respectively.

On substitution of Eqs.(8), (14) and (15) into Eq.(7) we obtain

$$G(\tau) = \sum_{a,n}\exp(-f_{an}\tau)\left|\sum_{b,l} d_{ab}^{(2)}(\beta_{DN})d_{b0}^{(2)}(\beta_{CH}^l)\exp(ib\alpha_{CH}^l)X_l^{(0)}X_l^{(n)}\right|^2, \tag{16}$$

where $f_{an} = 6D_\perp + a^2(D_{//} - D_\perp) + \lambda_n$.

Finally, the Fourier transformation of $G(\tau)$ gives the expression for the spectral density $J(\omega)$:

$$J(\omega) = 2\sum_{a,n}\frac{f_{an}}{f_{an}^2+\omega^2}\left|\sum_{b,l} d_{ab}^{(2)}(\beta_{DN})\, d_{b0}^{(2)}(\beta_{CH}^l)\exp(ib\alpha_{CH}^l)X_l^{(0)}X_l^{(n)}\right|^2. \tag{17}$$

For isotropic diffusion in which $D_{//} = D_\perp = D_0$, the orthogonality properties of $d_{ab}^{(2)}$'s can further simplify Eq.(17) to

$$J(\omega) = 2\sum_{n,b}\sum_{l}\frac{6D_0+\lambda_n}{(6D_0+\lambda_n)^2+\omega^2}\left|d_{b0}^{(2)}(\beta_{CH}^l)\exp(ib\alpha_{CH}^l)\, X_l^{(0)}\, X_l^{(n)}\right|^2. \tag{18}$$

It is noteworthy that Eqs. (17) and (18) formally take the form of distribution of the correlation times. However, unlike the empirical form of such distribution function which has been widely employed by many investigators, Eqs. (17) and (18) contain the distribution coefficients that depend not only on the position of the carbon of interest but also on the mode

of chain dynamics and the relevant rate constants. Hence they may be utilized for analyzing the ^{13}C spin-lattice relaxation time data to examine a proposed chain dynamics model.

Application to *n*-Undecane and *n*-Dodecane

The theory described thus far is now applied to interpret the spin-lattice relaxation data for ^{13}C in *n*-undecane and *n*-dodecane. It will be shown that we can determine the rate constants for direct conformational jumps in these molecules by comparing the observed T_1 data with those calculated from Eqs.(1) and (17) [or (18)]. Ignoring the rotamers arising from rotation of methyl groups at both ends of the chain, possible number of conformers for *n*-dodecane are 3^9 since the conformation around any given C – C bond in this molecule can be in any of the three states g^+, t, g^- and However, number of the conformers to be dealt with can be reduced by considering that ^{13}C T_1 data for *n*-alkanes in general show symmetry about the center of the molecule with T_1 being the longest for terminal group carbons and becoming shorter as we approach to the central atom. This means that we may focus our attention only on half of the carbon chain, which reduces the number of conformers we have to consider to $3^4 = 81$ for *n*-dodecane. The end methyl carbon is excluded from the consideration because its jump among three equal sites generates no new conformation of the molecule as a whole and the ^{13}C T_1 for this group is known to be affected also by a relaxation mechanism other than dipolar one.

Of course, one may deal with all these 81 conformations to calculate ^{13}C T_1 by taking advantage of the computer system with large memory and high-speed computing capability. However, further reduction in number of conformations is possible at this stage of calculation if we note that some of the 81 conformations mentioned above appear with so low frequencies that they can safely be ignored. One such conformation, which is energetically highly unfavorable, is that containing two *gauche* C – C bonds connected back to back[26]. For example, the conformation involving *ggt* is ignored although that involving *gtg* is allowed. Excluding all these unfavorable conformations, we are left with 21 conformations only as shown in Table 1. To calculate T_1 with these remaining 21 conformations, various Eulerian angles to describe the orientation of ^{13}C – ^{1}H bond of interest in these conformations must be specified in the coordinates system shown in Fig. 2. In Fig. 3, we show again the coordinates system appropriate to *n*-dodecane. Tetrahedral lattice vectors to depict the orientation of C – C bond and C–H bond are also shown in the same figure. The relative orientation of (X_N, Y_N, Z_N) coordinates with respect to (X_D, Y_D, Z_D) coordinates system is fixed spatially, giving $\beta_{DN} = 32.5°$ and $\gamma_{DN} = 0°$. The spatial orientations of C – C bonds and the

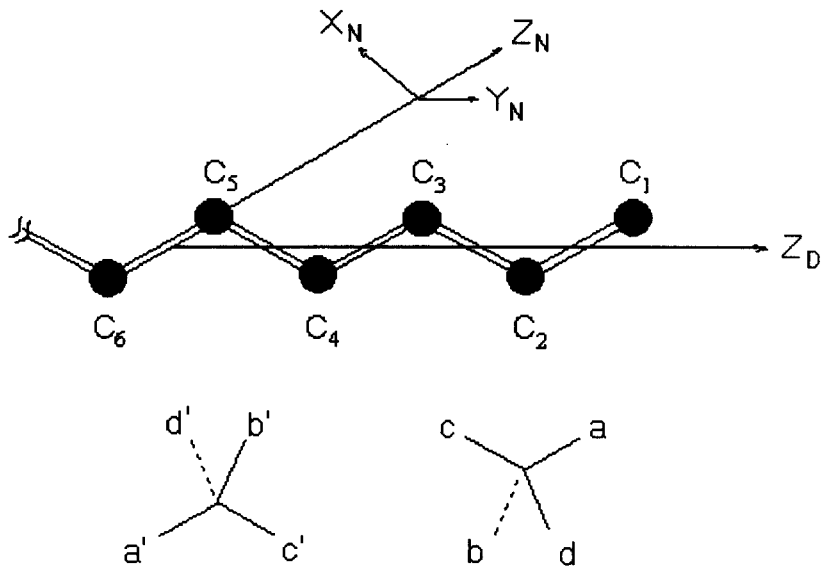

Fig. 3. Coordinate system and tetrahedral lattice used for calculation of dynamical parameters in n-dodecane

C – H bond of interest in 21 conformations can easily be described in tetrahedral lattice coordinates as shown in Table 1. Since the azimuthal and polar angles specifying the direction of each vector in tetrahedral lattice can be expressed in the N–coordinates as shown in Table 2, those for the C – H bond of interest can easily be found. For each carbon there are two protons attached to it, but only one, marked by an asterisk(*), of the two C – H bonds will be used for our calculation. Since the behaviors of chain in *n*-undecane and *n*-dodecane are expected to be statistically symmetrical about the central carbon or C–C bond, we have listed in Table 1 the conformations possible for only half of the chain. In principle any type of conformational jumps can occur between two of 21 conformers shown in Table 1, but it is highly likely that only those that require relatively low activation energy will actually take place. One of these is type II transition whose activation energy is lowered by cooperative rotational motions between two β-coupled C – C bonds. For example, the pair gauche generation and annihilation $ttt \leftrightarrow g^{\pm}tg^{\mp}$ and the gauche migration $g^{\pm}tt \leftrightarrow ttg^{\pm}$ are allowed. However, the direct jump such as $gtgt \rightarrow tgtg$ is not allowed. This transition should be considered as two direct jumps $gtgt \rightarrow tttt \rightarrow tgtg$ occurring sequentially. Special consideration should be given to terminal part of the chain such as ethyl and propyl group, because they are not so bulky, thus suffering less viscous drag forces when they swing

Table 1. Significant Conformations and the Directions of C-C and C-H Bonds in the Tetrahedral Lattice Coordinates.

Conformation	C-C Bond Conformation				C-C Bond Direction				C-H Bond Direction			
	C6-C5	C5-C4	C4-C3	C3-C2	C6-C5	C5-C4	C4-C3	C3-C2	C6-C5	C5-C4	C4-C3	C3-C2
1	g^+	t	g^+	t	d''	a	b'	a	c'	C	d''	d
2	g^+	t	t	g^+	d''	a	d''	b	c'	C	c'	a
3	g^+	t	t	t	d''	a	d''	a	c'	C	c'	c
4	g^+	t	t	g^-	d''	a	d''	C	c'	C	c'	b
5	g^+	t	g^-	t	d''	a	c'	a	c'	C	b'	b
6	t	g^+	t	g^+	c'	d	c'	b	b'	A	a'	d
7	t	g^+	t	t	c'	d	c'	d	b'	A	a'	a
8	t	g^+	t	g^-	c'	d	c'	a	b'	A	a'	b
9	t	t	g^+	t	c'	a	d''	a	b'	B	c'	c
10	t	t	t	g^+	c'	a	c'	d	b'	B	b'	a
11	t	t	t	t	c'	a	c'	a	b'	B	b'	b
12	t	t	t	g^-	c'	a	c'	b	b'	B	b'	d
13	t	t	g^-	t	c'	a	b'	a	b'	B	d''	d
14	t	g^-	t	g^+	c'	b	c'	a	b'	D	d''	b
15	t	g^-	t	t	c'	b	c'	b	b'	D	d''	d
16	t	g^-	t	g^-	c'	b	c'	d	b'	D	d''	a
17	g^-	t	g^+	t	b'	a	c'	a	d''	D	b'	b
18	g^-	t	t	g^+	b'	a	b'	c	d''	D	d''	a
19	g^-	t	t	t	b'	a	b'	a	d''	D	d''	d
20	g^-	t	t	g^-	b'	a	b'	d	d''	D	d''	c
21	g^-	t	g^-	t	b'	a	d''	a	d''	D	c'	c

Table 2. Polar and Azimuthal Angles for Each Tetrahedral Lattice Vector in N-Coordinate System.

Lattice Vector	a	b	c	d	a'	b'	c'	d'
α_{CH}	–	-120°	0°	120°	–	60°	180°	-60°
β_{CH}	0°	109.5°	109.5°	109.5°	180°	70.5°	70.5°	70.5°

through the solvent, that the type III jumps, besides type II, are expected to play a substantial role for them. Thus, we may think that terminal C – C bonds can also undergo the isolated type III jumps. As we have mentioned in the previous section, all the possible models within the frame of this picture must be tested to see whether they can reproduce the experimental data with good reliability over the observed range of temperature. Furthermore, we have to check if the rate constants obtained through this process are consistent with the physical reality that, the closer the C – C bond involved in conformational jump is located to the chain end, the larger the corresponding rate constant $\overline{R}_{ij}$ in Eq.(9) must be at a given temperature and that these rate constants should increase with temperature. The followings are the models we have tested for reproducing the experimental data in this work:

(*a*) all the jumps about C – C bonds, except $g^+ \leftrightarrow g^-$, are possible and mutually independent;
(*b*) only cooperative type II jumps are possible along the chain;
(*c*) only isolated type III jumps are possible about any C – C bond in the chain;
(*d*) all type II jumps involving any two β-coupled C – C bonds are possible throughout the chain but type III jumps are possible over the terminal two C–C bonds only including methyl and ethyl groups;
(*e*) the same model as described in (*d*) except for the possibility of occurrence of type III jumps extended over the terminal three C – C bonds covering methyl, ethyl, and propyl groups;
(*f*) the same as (*d*) except for the possibility of occurrence of type III jumps extended well over up to terminal four C – C bonds.

Case (*a*) is nothing but the London-Avitabile model which Chung *et al.*[2] have used to interpret their relaxation data for several *n*-alkanes dissolved in $CDCl_3$. Its reproducibility of the observed results was found to be reasonably good but the activation energies derived were found to be too low compared to that for single barrier crossing in small molecules. Thus it is very doubtful that the rotations about all C – C bonds may be assumed mutually independent. In Case (*b*) and (*d*) we failed to find a set of the rate constants that can reproduce the observed data with any acceptable accuracy. Furthermore, these two models predict completely wrong temperature dependence of the rate constants. The model (*c*) yielded a set of the rate constants that gave reasonable fittings with the experimental data at relatively low temperatures. But, in view of the fact that a rate constant defined for conformational jump about an inner C – C bond becomes larger than that about an outer C – C bond at higher temperatures we believe this model is physically unrealistic. Thus

are left with the model (*e*) and (*f*) which turned out to satisfy the criteria we have set up to find the correct model of chain dynamics for *n*-undecane and *n*-dodecane.

The calculational procedures for testing the validity of these two models are similar except for some minor differences, and we will illustrate the details of calculational method for *n*-dodecane employing the model (*e*). At this juncture some comments are in order regarding type II jumps involving C – C bonds protruding from the innermost carbon. (See Table 3.) Transitions involving the innermost C – C bond (for example, 11⇔3 and 11⇔19, also 11⇔7 and 11⇔15, which are characterized by the rate constants k_{11} and k_{12}) look ostensibly like the type III motions; however, they are not the type III motions. They are the type II motions which are β-coupled across the central carbon (or central C – C bond) to the rotation about the C – C bond in the other half of the chain.

In this case we have 40 different conformational transitions to consider (24 of them are of type II and 16 are of type III involving terminal groups) as shown in Fig. 4, to each of which we have to assign two rate constants, a forward and a reverse one. This means that we need to know 80 rate constants in all to describe the conformational interconversions in *n*-dodecane even at this simplified level, which is of course impossible considering that we cannot

Table 3. Definition of Basic Rate Constants for Conformational Interconversions in *n*-Undecane.

Rate Constants	Types of Conformational Transitions	Bonds Involved in Conformational Transitions
k_1	$t \rightarrow g^+, t \rightarrow g^-$	C3-C2
k_2	$g^+ \rightarrow t, g^- \rightarrow t$	C3-C2
k_3	$t \rightarrow g^+, t \rightarrow g^-$	C4-C3
k_4	$g^+ \rightarrow t, g^- \rightarrow t$	C4-C3
k_5	$ttt \rightarrow g^+tg^-, ttt \rightarrow g^-tg^+$	C5-C4, C4-C3, C3-C2
k_6	$g^+tg^- \rightarrow ttt, g^-tg^+ \rightarrow ttt$	C5-C4, C4-C3, C3-C2
k_7	$ttg^+ \rightarrow g^+tt, ttg^- \rightarrow g^-tt$ $g^+tt \rightarrow ttg^+, g^-tt \rightarrow ttg^-$	*C5-C4, C4-C3, C3-C2*
k_8	$ttt \rightarrow g^+tg^-, ttt \rightarrow g^-tg^+$	C6-C5, C5-C4, C4-C3
k_9	$g^+tg^- \rightarrow ttt, g^-tg^+ \rightarrow ttt$	C6-C5, C5-C4, C4-C3
k_{10}	$ttg^+ \rightarrow g^+tt, ttg^- \rightarrow g^-tt$ $g^+tt \rightarrow ttg^+, g^-tt \rightarrow ttg^-$	C6-C5, C5-C4, C4-C3
k_{11}	$t \rightarrow g^+, t \rightarrow g^-$	C6-C5 or C5-C4
k_{12}	$g^+ \rightarrow t, g^- \rightarrow t$	C6-C5 or C5-C4

obtain that many NMR relaxation data. Fortunately, we can introduce further simplifications regarding these rate constants as follows:

(*1*) The rate constants for 10 conformational interconversions that involve the type III jump $t \rightarrow g^{\pm}$ at the $C_2 - C_3$ bond may be considered to be all the same and denoted by k_1. The corresponding reverse rate constants may be considered likewise and will be denoted by k_2.

(*2*) Similarly, all the rate constants for 6 conformational interconversions that involve the type III jump $t \rightarrow g^{\pm}$ at the $C_3 - C_4$ bond may be considered to be all the same and denoted by k_3. The same is true for the corresponding reverse rate constants which will be denoted by k_4.

(*3*) The 24 type II transitions are listed in Table 3 along with their respective rate constants. Since the forward and reverse rate constants for *gauche migration* $g^+tt \rightarrow ttg^+$ and $g^-tt \rightarrow ttg^-$ involving a given set of three bonds may be considered to be all equal, eight rate constants need to be determined as shown in Table 3.

Even with the help of the above simplifying approximations we are still left with 12 rate constants to be determined at a given temperature while we have only four carbon T_1 data at our disposal. (Among the five available T_1 data the central carbon T_1 is reserved for calculating the diffusion constant D_0 for the rotation of the D-coordinates.) To tackle this difficulty we make use of the following relations valid for these rate constants[3,15] :

$$k_2 = k_1 \exp(\Delta E_{gt}/RT), \tag{19}$$

$$k_4 = k_3 \exp(\Delta E_{gt}/RT), \tag{20}$$

$$k_6 = k_5 \exp(2\Delta E_{gt}/RT), \tag{21}$$

$$k_7 = k_5 \exp\left(\Delta E_{gt}/RT\right), \tag{22}$$

$$k_9 = k_8 \exp(2\Delta E_{gt}/RT), \tag{23}$$

$$k_{10} = k_8 \exp\left(\Delta E_{gt}/RT\right), \tag{24}$$

$$k_{12} = k_{11} \exp(\Delta E_{gt}/RT)\ , \tag{25}$$

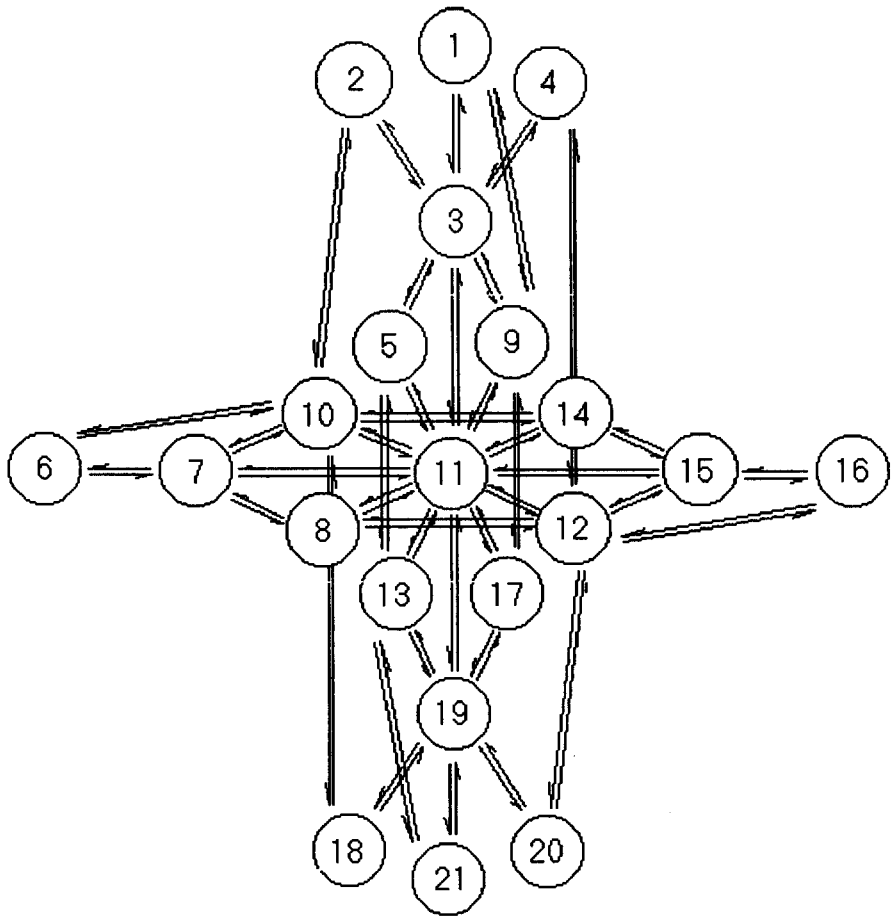

Fig. 4. Diagrammatical representation of conformational interconversions in n-dodecane. Each circled number corresponds to a conformation listed in Table 1 and each line between a pair of circled numbers represents a type II or type III interconversion between the corresponding two conformations

where ΔE_{gt} is the energy difference between the *gauche* and *trans* state of a C – C bond. These seven constraints reduce the total number of undetermined rate constants to just five. Since Eqs. (19) through (25) are nearly exact, the calculated temperature dependence of T_1 should serve as an important criterion for testing the validity of an assumed model of chain dynamics.

Similarly, we can also show that for *n*-undecane we again need to know five rate constants while only four T_1 data are available at a given temperature. Then, how can we

determine five rate constants uniquely despite the lack of enough number of data? One trick to get around this difficulty is that we solve the equations for determining these rate constants from measured T_1 data of both *n*-undecane and *n*-dodecane simultaneously, assuming that the two rate constants k_1 and k_3 for *n*-dodecane are, respectively, the same as the corresponding counterpart for *n*-undecane. This approximation can be considered quite reasonable because terminal ethyl and propyl group in *n*-dodecane are, respectively, expected to undergo the type III jumps with almost the same ease as their counterpart in *n*-undecane. This introduces two more constraints, enabling us to determine eight rate constants by making use of the eight T_1 data for *n*-undecane and *n*-dodecane at a given temperature. Also, we have assumed the rotational motion of the D-coordinates with respect to the laboratory-fixed coordinates obeys the isotropic rotational diffusion equation, because introduction of the anisotropy in the rotational diffusion constants was found to affect the final results only very slightly.

For testing the model (*f*) we have to introduce one more rate constant k_2' for type III jump about $C_4 - C_5$ bond. Since this additional rate constant cannot be directly found by solving the simultaneous equations used for testing the model (*e*), we solve these equations for varying ratio of k_2 / k_3. If this ratio is set to zero, the model reduces to the Case (*e*). Our calculations show that this model can give reasonable fittings with the observed data only when $k_2'/k_3 < 0.1$ and even these fittings gradually deteriorate with rise of temperature. Setting $k_2'/k_3 = 0.1$, we have calculated the magnitude of k_2' that yielded reasonable fittings with experimental data to find that it is even smaller than k_8, the rate constant for type II jump about two β-coupled C–C bonds, $C_6 - C_5$ and $C_4 - C_3$. This means that it is a good approximation to ignore type III jump about $C_4 - C_5$ for *n*-undecane and *n*-dodecane dissolved in $CDCl_3$ as far as interpretation of T_1 data is concerned.

Results and Discussion

Several rate constants involved in conformational interconversions such as listed in Table 3 have been calculated from T_1 data for *n*-undecane and *n*-dodecane reported by Chung *et al.*[2], and from the Arrhenius plot of thus obtained rate constants the activation energies for these motions have been evaluated. Calculations were performed numerically on a 486DX PC using the program written in FORTRAN specifically for the present purpose. The program was written such that input values for the rate constants are varied in small steps and at each step T_1 is calculated and compared with the observed one, which continues until the best agreement between calculated and observed T_1 is obtained.

Measured NOE factors for all the carbons were found to be close to the possible maximum (≈ 1.987) except for methyl carbon, which justifies our interpretation of ^{13}C relaxation data on the basis of dipolar relaxation mechanism. As expected, the NOE factors calculated by making use of our proposed model turned out to be very close to 2.0 for all the carbons over the entire range of investigated temperature.

For analysis of the observed data we begin by calculating the diffusion constant D_0 from T_1 value of the central carbon. Then we compute, using this D_0 and ΔE_{gt} ($\approx$3.36 kJ/mol) [27,28], ten rate constants (five for *n*-undecane and five for *n*-dodecane) by least-squares fitting of the T_1 data predicted by the assumed model with those measured for *n*-undecane and *n*-dodecane simultaneously at each given temperature. The Arrhenius type temperature dependence of thus obtained rate constants are shown in Figs. 5 and 6 from which the activation energy and the preexponential factor for each k_i have been evaluated and listed in Tables 4 and 5. Analytical expressions for these k_i's were in turn used to recalculate T_1's over the observed range of temperatures, resulting in good agreement between observed data and calculated values as shown in Figs. 7 and 8. We can also see that in the case of transitions involving terminal ethyl or propyl unit the calculated rate constants for the type III conformational changes are larger than those for type II transitions as we expect. The rate constants k_{11} and k_{12}, which correspond to the type II motions involving the central carbon or C – C bond which is β-coupled to another C – C bond in the other half of the chain, are found to be smaller than the rest of the rate constants almost by two order and their contributions to T_1 are thus negligible in our case. As we can see from Tables 4 and 5, for the type III motions involving terminal groups only, the rate constants are of the order of 10^{10} sec^{-1} while those for type II transitions are smaller than this nearly by one order. However, it is also found that the latter increases more rapidly than the former as temperature rises. The activation energies of most conformational transitions were found to be approximately in the range of 12 –20 kJ/mol which is comparable to those associated with the one bond rotation in small molecules (*ca.* 12 kJ/mol [8,9]. Also, by making use of thus found expressions for the rate constants we have calculated the time-dependent orientational correlation function $G(\tau)$ for each ^{13}C – ^{1}H vector in *n*-undecane and *n*-dodecane and the results are shown in Figs. 9 through 12. We see from this that the largest contribution to $G(\tau)$ comes from the overall molecular rotation (that is, the motions of the D-coordinates with respect to the laboratory-fixed coordinates) but the contribution from segmental motions gradually increases as we move toward the terminal carbon. The calculated time-dependence of these correlation functions are all comparable with those reported previously for other hydrocarbons[22-24] and may be regarded as reasonable despite the approximations involved in our model. The E_a values listed in Tables 4 and 5 reflect the activation energies for conformational inter-

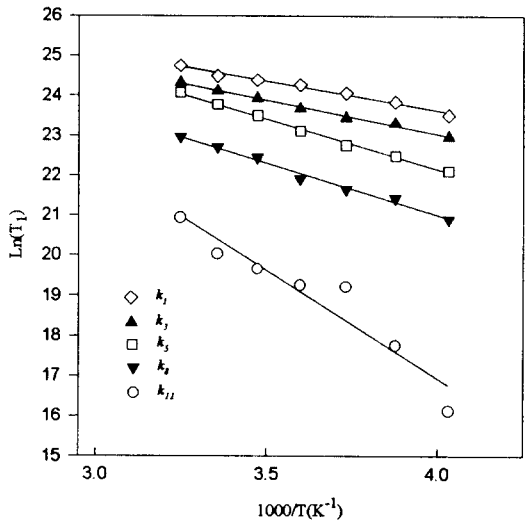

Fig. 5. The Arrhenius plot of calculated rate constants for conformational interconversion in n-undecane

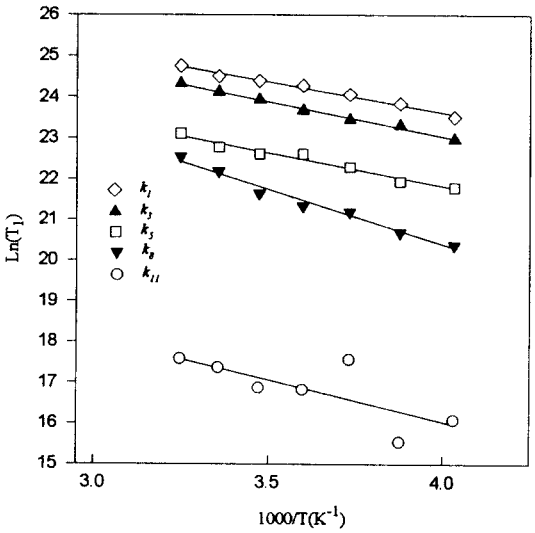

Fig. 6. The Arrhenius plot of calculated rate constants for conformational interconversion in n-dodecane

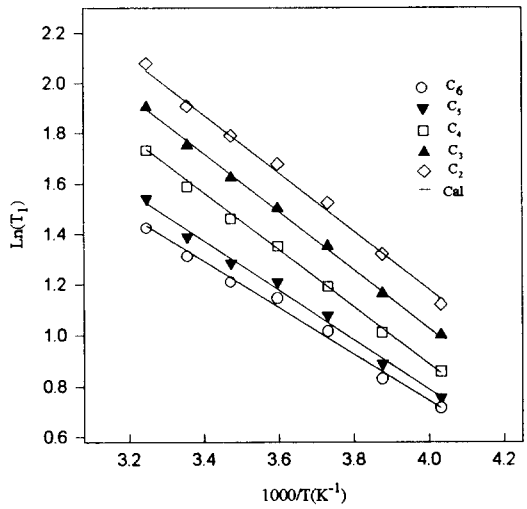

Fig.7. Comparison of overserved and calculated ^{13}C T_1's for each carbon of *n*-undecane

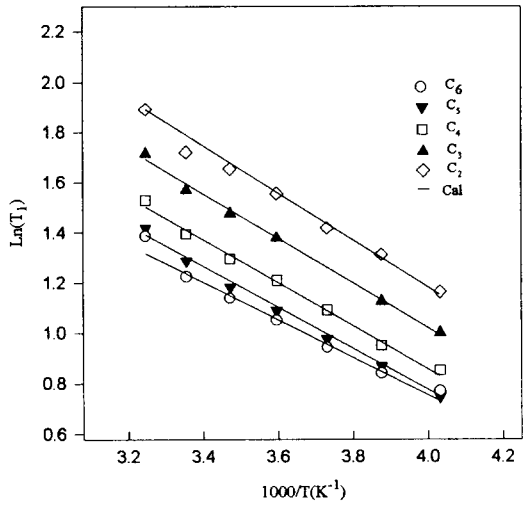

Fig.8. Comparison of overserved and calculated ^{13}C T_1's for each carbon of *n*-dodecane

conversions occurring in *n*-undecane and *n*-dodecane in their $CDCl_3$ solution. In principle, if the spin-lattice relaxation time data are measured using several other solvents and the corresponding relaxation parameters are obtained for them by making use of the model adopted in this paper, then the activation energies for segmental motions in these solvent may be evaluated and this will enable us to understand the solvent effect on segmental motions in *n*-undecane and *n*-dodecane. Investigation along this line is underway in our laboratory and the results will be reported sooner or later.

Table 4. Calculate Diffusion Constants and Rate Constants for Conformational Transitions in *n*-Undecane from the Model with Anisotropic Overall Rotation at Various Temperatures.

T (K)	Diffusion Constants and Rate Constants (in unit of 10^9 sec^{-1})					
	D_0	k_1	k_3	k_5	k_8	k_{11}
248	14.6	16.2	9.45	4.04	1.20	0.0101
258	16.4	22.5	13.3	5.90	2.05	0.0512
268	19.8	28.2	15.2	7.66	2.55	0.222
278	22.5	34.7	19.1	10.9	3.30	0.231
288	24.0	39.0	24.7	16.1	5.65	0.347
298	26.6	43.3	29.7	21.2	7.29	0.503
308	30.1	56.0	36.6	28.7	9.39	1.24
E_a^*	7.60	12.2	14.0	20.7	20.7	
$A^\#$	0.58	6.48	8.74	96.4	43.3	

* Activation energies are in the unit of kJ/mol

\# Pre-exponential factors are in the unit of 10^{12} sec^{-1}

Table 5. Calculated Rate Constants for Conformational Transitions in n-Undecane and n-Dodecane

T (K)	Diffusion Constants and Rate Constants (in unit of 10^9 sec^{-1})					
	D_0	k_1	k_3	k_5	k_8	k_{11}
248	15.1	16.2	9.45	2.91	0.711	0.0096
258	16.6	22.5	13.3	3.36	0.962	0.0056
268	18.4	28.2	15.2	4.82	1.60	0.0421
278	20.5	34.7	19.1	6.63	1.86	0.0201
288	22.3	39.0	24.7	6.61	2.52	0.0211
298	24.3	43.3	29.7	7.75	4.30	0.0347
308	27.2	56.0	36.6	10.8	6.20	0.0428
E_a^*	6.80	12.2	14.0	13.7	21.0	
$A^{\#}$	0.29	6.48	8.74	1.95	35.5	

Acknowledgement.

This research was supported by a grant (Project No. BSRI 97-3414) from the Basic Science Research Institute Program, Ministry of Education, Korea, 1997.

REFERENCES

1. J. R. Lyerla, Jr. and T. T. Horikawa, *J. Phys. Chem.* **80** (1976) 1106.
2. J. Y. Chung, J. W. Lee, H. Pak and T. Chang, *Bull. Kor. Chem. Soc.* **13** (1992) 296.
3. R. E. London and T. Avitabile, *J. Am. Chem. Soc.* **99** (1977) 7765.
4. F. Liu, W. J. Horton, C. L. Mayne, T. Xiang and D. M. Grant, *J. Am. Chem. Soc.* **114** (1992) 5281.
5. M. M. Fuson, M. S. Brown, D. M. Grant and G. T. Evans, *J. Am. Chem. Soc.* **107** (1985) 6695.
6. M. Baldo and A. Grassi, *Magn. Reson. Chem.* **27** (1989) 533.
7. D. Wallach, *J. Chem. Phys.* **47** (1967) 5258.
8. F. Heatley, *Prog. NMR. Spectry.* **13** (1979) 47.

9. E. Helfand, *Science*, **226**(1984) 647.
10. R.Daudel *et al.* , *Structure and Dynamics of Molecular Systems-II* (Reidel Publishing Company, 1986) *pp.* 129-154.
11. G. Lipari and A. Szabo, *J. Am. Chem. Soc.* **104** (1982) 4546.
12. H. G. Hertz, *Prog. NMR. Spectry.* **16** (1983) 115.
13. D. E. Woessner, *J. Chem. Phys.* **42** (1965) 1885.
14. H. Versmold, *J. Chem. Phys.* **58** (1973) 5649.
15. R. J. Wittebort and A. Szabo, *J. Chem. Phys.* **69** (1978) 1772.
16. Y. K. Levine, P. Partington and G. C. K. Roberts, *Mol. Phys.* **25** (1973) 497.
17. F. A. Bovey and L. W. Jelinski, *J. Phys. Chem.* **89** (1985) 571.
18. J. Skolnick and E. Helfand , *J. Chem. Phys.* **72** (1980) 5489.
19. E. Helfand and J. Skolnick, *J. Chem. Phys.* 77 (1982) 5714.
20. E. Helfand, Z. R. Wasserman and T. A. Weber, *Macromolecules*, **13** (1980) 526.
21. D. J. Gisser, S. Glowinkowski and M. D. Ediger, *Macromolecules*, **24** (1991) 4270
22. G. T. Evans and D. C. Knauss, *J. Chem. Phys.* **72** (1980)1504.
23. T. Xiang, F. Liu and D. M. Grant, *J. Chem. Phys.* **95** (1991) 7576.
24. G. D. Smith and D. Y. Yoon, *J. Chem. Phys.* **100** (1994) 649.
25. M. E. Rose, *Elementary Theory of Angular Momentum* (John Wiley & Sons, Inc., New York, 1957).
26. The computer simulation study byJ. H. R Clarke and D. Brown [*Mol. Phys.* **58**(1986)815] show that for *n*-hexane the sum of the concentrations of *tgg* and *ggg* is 1% at 200 K and 4% at 300 K.
27. A. L. Verma, W. F. Murphy and H. J. Bernstein, *J. Chem. Phys.* **60** (1974) 1540.
28. P. J. Flory, *Statistical Mechanics of Chain Molecules*, (John Wiley & Sons. Inc., New York, 1969).